# Solvent Structure Around Lanthanoids(III) Ions in Liquid DMSO as Revealed by Polarizable Molecular Dynamics Simulations

Enrico Bodo,*,† Veronica Macaluso,†,¶ and Riccardo Spezia*,‡

*Dept. of Chemistry, University of Rome "La Sapienza", Italy, and LAMBE CNRS UMR8587, Universite dEvry val dEssonne, Blvd F. Mitterrand, Bat̂ Maupertuis, 91025 Evry, France*

E-mail: enrico.bodo@uniroma1.it; riccardo.spezia@univ-evry.fr

*To whom correspondence should be addressed

†Dept. of Chemistry, University of Rome "La Sapienza", Italy

‡LAMBE CNRS UMR8587, Universite dEvry val dEssonne, Blvd F. Mitterrand, Bat̂ Maupertuis, 91025 Evry, France

¶Present address: LAMBE CNRS UMR8587, Universite dEvry val dEssonne, Blvd F. Mitterrand, Bat̂ Maupertuis, 91025 Evry, France

**Abstract**

We present a study of the solvation of lanthanoid(III) ions in liquid dimethylsulfoxide (DMSO) using molecular dynamics simulations employing a newly developed polarizable force field. The van der Waals (vdW) parameters were obtained for $La^{3+}$ and $Lu^{3+}$ (the first and the last in the lanthanoids(III) series) using *ab initio* data. The parameters of the other ions can be extrapolated based on physical considerations without additional (and costly) quantum chemistry calculations. This extrapolation procedure has been successfully applied to $Gd^{3+}$. The outcomes of our simulations turn out to be in agreement with both the experimental data available in the literature and the *ab initio* results. A small adjustment of the vdW parameters further increases the agreement with experiments and has allowed us to provide structures, geometrical parameters and coordination numbers. For heavy lanthanoids (Gd and Lu) we obtain clearly an 8-fold coordination, with a distorted square anti prism (SAP) geometry in agreement with EXAFS and XANES experiments; for the $La^{3+}$ ion, our force field predicts a mixed situations with both the 8-fold SAP and 9-fold geometry where the SAP structure is capped by a ninth molecule added over one face.

## Keywords

Lanthanoids, Organic Solvents, Solvation Structure, Molecular Dynamics Simulations, Polarizable Force Fields

## Introduction

Lanthanoid(III) ($Ln^{3+}$) ions form an almost unique chemical series whose elements bear the same oxidation state and are soluble in different polar solvents, from water[1] to organic solvents[2] and ionic liquids.[3] When an ion is dissolved in a polar solvent it generally structures the molecules around itself forming relatively stable structures whose shape and size depend on the charge of the ion, on its radius and on the polar properties of the solvent.[4,5] The $Ln^{3+}$

series forms a unique example to investigate the solvation behavior along a chemical series in which each element bears the same charge but with changing ionic radii (they decrease as the atomic number increases), and thus experimental studies have often investigated how the solvation properties vary when moving from light to heavy elements in the series.[1,2,6–15]

Theory represents an invaluable help in understanding from a microscopic point of view the changing of these properties, as it has been the case, for example, for the hydration of $Ln^{3+}$ ions.[16–23]

While hydration of $Ln^{3+}$ ions has been explored by many experimental and theoretical studies,[1] the solvation in organic solvents remains much less investigated. The study of $Ln^{3+}$ in organic solvents is important because they can be involved in separation/decontamination applications so that, by understanding the molecular basis of solvation in non-aqueous solvents, it may be possible to devise new solvent extraction techniques. Polar organic solvents like dimethylsulfoxyde (DMSO) were used in some experimental studies, investigating the structure of DMSO around the $Ln^{3+}$ ions[2,15] also in presence of additional ligand molecules as, for example, the complexation of $Ln^{3+}$ ions by different polyamines.[24–27]

Recent experimental determinations[15,28] have proposed that the DMSO forms a regular shell of eight oxygen atoms surrounding the central ion for all the lanthanoid(III) series. The spectroscopic and crystallographic studies of lanthanoid(III) iodides revealed that lanthanoid(III) ions have an eight-coordinated configuration in liquid DMSO that is similar to the solid state.[2,11,24] These works, in particular, have shown that the coordination number does not seem to change along the series, although the decrease in the mean Ln–O distances is greater than expected on the basis of existing ionic radius data for eight-fold structures.[11] Anyhow, the coordination state of $Ln^{3+}$ ions in DMSO solution is still controversial, since EXAFS can have a $\pm$ 1 accuracy in determining the coordination numbers. Furthermore, other studies have suggested some changes in the average coordination number along the series,[25] as reported in FT-IR studies of lanthanoid trinitrates in the presence of DMSO in anhydrous acetonirile.[29] This result was also confirmed in a very recent investigation dealing

with apparent molar volumes and compressibilities of $Ln^{3+}$ trifluoromethanesulfonates in DMSO.[30] In addition, gas phase *ab initio* calculations by us[31] have shown that, probably, the first coordination shell is made by a more complex environment where a regular structure of eight oxygen atoms coexist with a structure with nine oxygen atoms, the latter being substantially iso-energetic with the former.

Molecular dynamics of ions in liquid solvent is the method of choice to understand deeply the solvation properties at finite temperature.[32,33] This method is able to provide a microscopic picture of ion solvation also taking into account dynamical processes that can occur, and thus also complex solvation situations in which thermal coexistence between two (or more) coordination numbers can be revealed.[20,34,35] In this work we have addressed the question of $Ln^{3+}$ solvation in DMSO by polarizable molecular dynamics simulations. Highly charged ions such $Ln^{3+}$ should be treated with polarizable force fields, as largely reported in the case of water.[17,18]

To this end we have developed a polarizable potential for $La^{3+}$ and $Lu^{3+}$ by matching the geometry of small $La^{3+}$ and $Lu^{3+}$-DMSO clusters in the gas phase. We then have obtained the non-electrostatic terms of $Gd^{3+}$-DMSO interaction potential by assuming a linear dependence of parameters across the series, thus avoiding expensive and complex ($Gd^{3+}$ is open shell) quantum chemistry calculations. This approach is justified by the well known fact that many solvation properties directly depends on ionic radii that decrease almost linearly across the series.[14] Results were compared with available experiments on DMSO structuration around the $Ln^{3+}$ ions and microscopic details of solvation are then provided.

# Computational details

Molecular dynamics simulations have been performed by means of the polarizable Amoeba[36] force field (FF) and the Tinker package.[37] Amoeba is a universal and transferable force field

so that, in principle, the new parameters will be easily usable for other studies whereby the Amoeba force field can be applied to different molecular scales from isolated inorganic molecules to bio-molecules.[38–46] In addition, instead of relying on "in house" codes and methods,[47] here we tried to adopt a user-friendly well distributed code that could therefore allow anyone to use and implement the new potentials in different systems. In this work, we have considered only three ions in the lanthanoid(III) series: $La^{3+}$, the first atom of the series, $Lu^{3+}$, the last atom of the series, and $Gd^{3+}$ that is in the middle of the series. $La^{3+}$ and $Lu^{3+}$ have been used to calculate the potential, while $Gd^{3+}$ has been used as test case to check for the FF extrapolation procedure. By limiting ourselves to two ions and extrapolating the potentials along the series, we purposely avoid the difficulty of performing the tricky, open-shell, *ab initio* calculations that would be needed to create the FF for the all the other lanthanoid(III) ions. As revealed in a number of studies of these ions in water, such choice is often enough to provide a correct trend of different properties.[14,20,21,48]

Each ion is immersed in a cubic box containing 68 DMSO molecules and, after an initial equilibration in the NpT ensemble at room conditions (T = 298 K and p = 1 atm, using the Berendsen thermostat), a fixed side length of 20.218 Å was set for the following NVT simulations. A cutoff of 9.0 Å for vdW interactions was used. Electrostatic has been evaluated by the regular Ewald method using the same cutoff. The production was carried out for at least 4 ns in the NVT ensemble (using a Berendsen thermostat and an integration step of 1 fs) for each of the cation/potential combinations that will be presented in the following. For the La-DMSO case, additional simulations starting from different initial conditions have been performed for a total of further 8 ns of simulation time.

The FF used in the present work, for which we have developed parameters for $Ln^{3+}$ ions, is the well known Amoeba potential, that we will briefly recall in the following, in particular for the non-bonded parameters. In Amoeba the total FF energy is expressed as a sum of 8 terms

$$U = U_{\text{bond}} + U_{\text{angle}} + U_{\text{b-a}} + U_{\text{oop}} + U_{\text{torsion}} + U_{\text{vdW}} + U_{\text{ele}} + U_{\text{ind}} \quad (1)$$

where the first 5 terms describe the topologically bonded interactions and the last 3 the long-range interactions. The bonded interactions are given by a quartic expansion in distance, a sextic expansion over the angular variable, a linear bond-angle cross term and a quadratic out-of-plane potential. The usual Fourier 3-term expansion of the torsional energy is also added. The vdW interaction potential in the Amoeba force field is given by a "soft" 7-14 potential (instead of the traditional Lennard-Jones 6-12 one):

$$U_{\mathrm{vdW}}(ij) = \epsilon_{ij} \left( \frac{1.07}{\rho_{ij} + 0.07} \right)^7 \left( \frac{1.12}{\rho_{ij}^7 + 0.12} - 2 \right) \tag{2}$$

where $\rho_{ij}$ is $r_{ij}/r_{ij}^0$. The vdW parameters are obtained through the following combination rules

$$\epsilon_{ij} = \frac{4\epsilon_{ii}\epsilon_{jj}}{(\sqrt{\epsilon_{ii}} + \sqrt{\epsilon_{jj}})^2}, \quad r_{ij}^0 = \frac{(r_{ii}^0)^3 + (r_{jj}^0)^3}{(r_{ii}^0)^2 + (r_{jj}^0)^2} \tag{3}$$

The centers of the vdW interactions are the atomic centers, with the exception of hydrogens for which the vdW center is shifted along the X-H bond by a fixed "reduction factor".

The electrostatic potentials in Amoeba include both permanent and induced multipoles interaction energies. Each center is associated with a point charge, a dipole and a quadrupole for a total of 5 distinct multipole components per atom (see[36] for details). The induced multipole at each site is then obtained from the electric field at that site using the Thole damped interaction method.[49] The smearing function in Amoeba is

$$\rho = \frac{3a}{4\pi} \exp(-au^3) \quad \text{with} \quad u = \frac{r_{ij}}{(\alpha_i \alpha_j)^{1/6}} \tag{4}$$

with a universal damping factor $a = 0.39$ and $\alpha$ the atomic polarizability.

The calculation of free energies has been performed by the umbrella sampling method where one spatial coordinate (the La-O distance) has been restrained using an harmonic potential (with a constant of 300 kcal/Å$^2$) for 83 increasing values starting from 2.4 up to 7.0 Å. One NVT simulation of 10 ps has been carried out at each distance (2 ps were left for

structural relaxation). The free energy profile (Potential of Mean Force) has been estimated through the Weighted Histogram Analysis Method (WHAM) as implemented in ref.[50] and the code of ref.[51] The final free energy profile has been corrected using the entropic term for spherical systems:[52,53]

$$T\Delta S(r) = 2k_B T \log(r/r_0) \tag{5}$$

where $r_0$ is the distance where the PMF is zero yielding the free energy correction with respect to the minimum of the PMF.

## Force field development

The force field parameters of DMSO have been determined by *ab initio* calculations on an isolated molecule. Geometric optimization at the HF/6-31G* has been followed by a frequency evaluation. The parameters (equilibrium distances and forces) obtained in this way for bonds and angles are substantially the same as those reported in the standard set of parameters of the amoeba09 FF. The charge distribution, ESP fitting charges and multipole calculation has been performed at the MP2/6-311++G(2d,2p) level. The resulting partial atomic charges are -0.33217 for C, 0.92255 for S, -0.70269 for O and 0.07408 for H. The dipole moment of the resulting molecule at the MM level is 4.116 D which matches well the *ab initio* value of 4.08 D and near the experimental value of 3.96 D.[54]

In order to test the DMSO model potential, a cell with a side length of 20 Å containing 68 DMSO molecules has been equilibrated at room conditions in the NpT ensemble using the Berendsen thermostat/barostat. The average density of the resulting pure liquid DMSO was 1.074±0.01 g/cm$^3$ (that compares well with the experimental value of 1.091 g/cm$^3$[54]) and the self-diffusion coefficient turned out to be $5.1 \cdot 10^{-10} m^2 s^{-1}$ that compares less favorably with the experimental value of $9.5 \cdot 10^{-10} m^2 s^{-1}$ probably because of the combined effect of the Berendsen thermostat and the small size of the cell, but is sufficiently accurate to study DMSO structural properties around highly charged ions.[55,56] The dipole polarizabilities of

the lanthanoid(III) ions have been taken from the fully relativistic calculations of ref.[57] and are 1.13, 0.82 and 0.61 Å$^3$ for $La^{3+}$, $Gd^{3+}$ and $Lu^{3+}$ respectively.

The parameters of the short range non electrostatic (vdW) interaction potential $\epsilon_{ii}$ and $r^0_{ii}$ for $La^{3+}$ and $Lu^{3+}$ have been obtained by a trial and error procedure starting from a reasonable ansatz reported by OPLS force field[58] and optimizing the "homonuclear" vdW parameters of the $Ln^{3+}$ ion in order to reproduce geometry of $Ln^{3+}(DMSO)_n$ clusters obtained by the *ab initio* calculations in the gas phase. This procedure leaves unchanged the original Amoeba vdW parameters for the Oxygen atom therefore preserving the transferability of the resulting FF.

The *ab initio* data (La-O distances and interaction energies) for the $La^{3+}$ have been taken from the calculations reported in ref.[31] For $Lu^{3+}$ we have optimized the clusters with 1, 4, 6 and 8 DMSO molecules using the B3LYP/6-31+G(d) combination and the Small Core ECP and basis [59] for Lu. No *ab initio* calculations were performed for $Gd^{3+}$ because of the difficulty in converging HF/DFT solution on such a high spin system. The vdW parameters were refined in a trial and error procedure using only the $Ln^{3+}$-DMSO, $Ln^{3+}(DMSO)_4$ and $Ln^{3+}(DMSO)_6$ *ab initio* results, while the $Ln^{3+}(DMSO)_8$ has been used as a reference test of the goodness of the derived potential. The La-O distances and their *ab initio* counterparts are reported in Table 1 along with the best fitting potential parameters. We notice that we have a set of parameters that reproduces the $Ln^{3+}$-DMSO systems and another that is able to reproduce both $Ln^{3+}(DMSO)_4$ and $Ln^{3+}(DMSO)_6$ systems. The latter is then used for the n = 8 clusters (to check the robustness of the parameters) and for the liquid phase.

Using these potentials for the above mentioned clusters, the $Ln^{3+}$-O distances resulting from the *ab initio* geometries were reproduced within 0.03 Å of accuracy and the *ab initio* interaction energies (defined as the difference between the energy of the complex and the energy of the separated molecular constituents) of the Ln-DMSO complex were reproduced to roughly 10%. As shown in the Table 1, our Amoeba force field is able to grasp both the geometric and energetic feature of the $La^{3+}(DMSO)_8$ cluster even though it was not used in

the refinement of the force field parameters.

**Table 1: Average $Ln^{3+}$-O distances from *ab initio* and Amoeba geometric optimization with the vdW parameters sets (with potential (2) results reported in parenthesis). We have also reported the interaction energies as computed by MM (with potential (2) results reported in parenthesis) and QM methods.The parameters reported in bold are those that have been used for the simulation of the liquid phase (with potential (2) parameters in parenthesis)**

| | $La^{3+}$[DMSO] | $La^{3+}$[DMSO]$_4$ | $La^{3+}$[DMSO]$_6$ | $La^{3+}$[DMSO]$_8$ |
|---|---|---|---|---|
| La-O average distance in Å | | | | |
| DFT | 2.01 | 2.29 | 2.41 | 2.52 |
| Amoeba | 2.04 | 2.31 (2.26) | 2.41 (2.36) | 2.52 (2.48) |
| Cluster interaction energy in kcal/mol | | | | |
| DFT | -219 | -539 | -645 | -729 |
| Amoeba | -178 | -488 (-509) | -656 (-688) | -692 (-714) |
| vdW parameters in Å and kcal/mol | | | | |
| $r^0$ | 4 | **4 (3.9)** | **4.0 (3.9)** | **4.0 (3.9)** |
| $\epsilon$ | 1.2 | **2.5** | **2.5** | **2.5** |

| | $Lu^{3+}$[DMSO] | $Lu^{3+}$[DMSO]$_4$ | $Lu^{3+}$[DMSO]$_6$ | $Lu^{3+}$[DMSO]$_8$ |
|---|---|---|---|---|
| Lu-O average distance in Å | | | | |
| DFT | 1.88 | 2.09 | 2.22 | - |
| Amoeba | 1.88 | 2.09 | 2.22 (2.20) | 2.37 (2.32) |
| Cluster interaction energy in kcal/mol | | | | |
| DFT | -257 | -607 | -700 | -730 |
| Amoeba | -210 | -580 | -707 (-729) | -778 (-797) |
| vdW parameters in Å and kcal/mol | | | | |
| $r^0$ | 4 | 3.67 | **3.62 (3.53)** | **3.62 (3.53)** |
| $\epsilon$ | 1.68 | 1.7 | **2.5** | **2.5** |

As we shall show in the following, the potentials that have been determined so far by comparison with the *ab initio* structural data slightly overestimate the Ln-O distances in solution when compared to experiments. Since for $La^{3+}$ this is the key factor in determining also the shell structure, we have also tested the same potentials above with a small (2.5%) reduction of the effective radius $r^0$ (see Table 1 where the values for the "rescaled" potentials

are given in parenthesis). While these "rescaled" potential models are unable to reproduce exactly the structural features of the gas-phase clusters above, nevertheless we report the results stemming from them because they turn out to be more accurate in reproducing the solution structure in liquid DMSO. We will have thus results for the original potentials and for the "rescaled" ones (labeled (1) and (2) respectively in the following).

The potential parameter $r^0$ for $Gd^{3+}$ has been interpolated using the ones obtained for $La^{3+}$ and $Lu^{3+}$ based on the well known linear decrease of the ionic radii of lanthanoids ions.[60] In this respect the simulations of $Gd^{3+}$ have been used as a test case in order to prove that, using the above procedure, we have parametrized a "universal" Amoeba force field for all the lanthanoid ion series. The force field parameters for $Gd^{3+}$ turned out to be $r^0 = 3.77$ Å ($r^0 = 3.67$ in potential (2)) and $\epsilon = 2.5$ kcal/mol. A tinker configuration file (a template example for the $La^{3+}$ ion in DMSO) is reported in the supporting information.

# Results

As an expected result, the DMSO solvent molecules are well structured around the ion, due to the strong electrostatic forces exerted by the ion and the sizable dipole moment of DMSO. By taking the trajectory for $La^{3+}$ as an example and putting the positive ion in the center, we can easily represent the average density of the solvent's oxygen atoms, as shown in Figure 1, where the density is cut at about 75% of its maximum value. An almost regular structure stems from the dynamics and it clearly emerges that the first solvation shell is strongly localized around the central ion. Very similar situations are obtained in the case of $Lu^{3+}$ and $Gd^{3+}$ ions.

In Figure 2 we report the radial distribution functions (RDF) of the $Ln^{3+}$-O distances within the first 3.5 Å and the corresponding integral as to give the coordination number (CN). This data has been collected on 4 to 6 ns of trajectory depending on each ion. We can see that the CN for $La^{3+}$ is between 8 and 9 while those arising from the $Lu^{3+}$ and $Gd^{3+}$ are

precisely 8. This change is clearly due to the diminished ionic radii of $Lu^{3+}$ and $Gd^{3+}$ with respect to $La^{3+}$. Only for $La^{3+}$ we report RDFs of both potential(1) and (2), because, as we will see, there are interesting differences. While for $Lu^{3+}$ and $Gd^{3+}$ the differences in the Ln-O RDF is minimal by changing potential (1) with (2) and we see only a slight adjustment of the peaks position to lower distances (see Table 2), the situation is different for $La^{3+}$. Upon changing the potential (1) with (2) we see that the RDF not only shifts at smaller distances, but also substantially changes its shape by becoming more compact. Accordingly, the CN diminishes from 8.6 to 8.4 thereby signaling a somewhat different shell structure for the very first solvating oxygen atoms. It is important to remark that while for the two "smaller" lanthanoid ions we obtain a purely 8-fold coordination, for $La^{3+}$ with both potential models we get a mixed coordination due to the coexistence of 8 and 9-fold coordination shells. This interesting result confirms our previous findings from accurate gas phase calculations[31] that have shown how the free energy difference between a cluster containing 9 DMSO molecules directly bound to the central ion and one made by 8 DMSO molecules directly bound and one DMSO in second shell is very small and comparable to RT at room temperature.

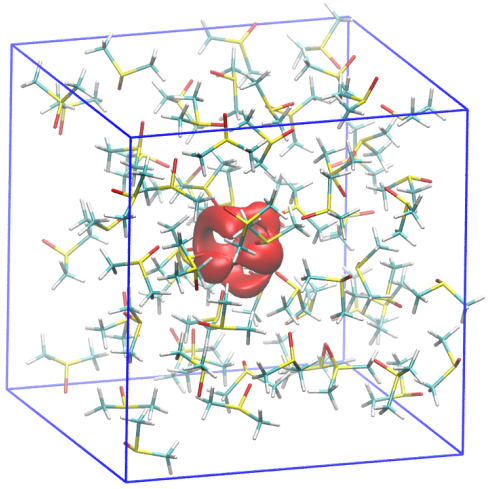

Figure 1: Density of the oxygen atoms in the unit cell cut at about 75% of the maximum value

In Table 2 we report the average Ln-O distances for the three different ions as it stems

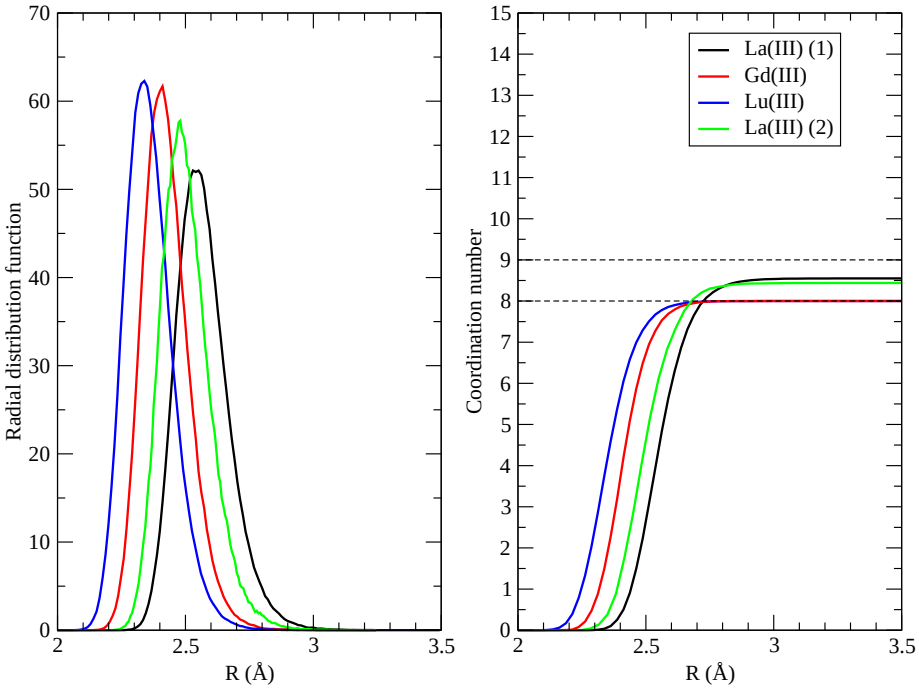


Figure 2: Radial distribution functions for the $Ln^{3+}$-O distance (left) and relative integral or coordination number (right).

from 4 ns trajectories, as well as the maximum of the Ln-O radial distribution functions. First we comment results obtained by potential (1) that is directly derived from ab initio calculations. As we can see, the simulation distances obtained are in fairly good agreement with the corresponding experimental data with an average error of no more than 3%. Note that the difference between the average and the maximum of the distribution is about 0.02 Å for $Lu^{3+}$ and $Gd^{3+}$, while is significantly larger for $La^{3+}$ because of the coexistence of 8-fold and 9-fold structures that, in turn, gives rise to a sizable broadening of the RDF. This is due to the fact that the $La^{3+}$ ion is able to accommodate 9 molecules of DMSO in the first solvation shell while the experimental data would tend to exclude this case.[28] We also note that Persson et al.[2] have analyzed the data from the EXAFS experiments using a non-symmetric distribution so that we can compare the differences between the average and the maximum of the distributions: less then 0.02 Å is reported, thus suggesting that the solvation shell is probably more compact than our findings with potential model (1). Nevertheless, considering that the employed force field has not been fitted on these experimental observables but, instead, obtained by purely *ab initio* considerations the result and the agreement between the distances reported in Table 2 is remarkably good.

In Table 2 we have also reported the results arising from the second model potential, labeled (2), that has a reduced van der Waals radius by 2.5%. The "rescaled" potentials provide results that, in turn, better fit the experimentally determined $Ln^{3+}$-O profiles and geometries. It is worth noting that in the case of $La^{3+}$, though using the potential model (2), that gives a much better agreement with experimental data, we still obtain a mixed 8/9-fold coordination shell. Obviously, such a reduced-radius model is not able to fit correctly the gas-phase structures of the cluster reported in Table 1 where it produces distances that are too short by about 3% with respect with the *ab initio* results. Assuming that the coordinated oxygen "radius" is the same adopted in ref.,[14] i.e. 1.35 Å, we can easily calculate from the potential (2) data Table 1 in the ionic radii of the $Ln^{3+}$ ions that are 1.15, 1.03 and 0.98 Å for $La^{3+}$, $Gd^{3+}$ and $Lu^{3+}$ respectively. In water the following effective radii for the same atoms

were reported[14] 1.250 Å; 1.050 Å and 0.995 Å. The values we obtained for $Gd^{3+}$ and $Lu^{3+}$ are very similar, while for $La^{3+}$ in DMSO we have a smaller value. This is not surprising since, for the latter, only the 9-fold structure is populated in water, while in DMSO we have a coexistence of 8- and 9-fold geometries and it is known that an 8-fold geometry corresponds to smaller ionic radii.[21,60]

**Table 2: La-O distances, in Å, as obtained by the simulations using the *ab initio* adjusted van der Waals parameters, Potential(1), and the rescaled ones, Potential(2). EXAFS K-edge and $L_3$-edge data of ref[2] and XANES data of ref[15] are reported for comparisons. In the case of simulation and EXAFS data we report the barycenter and, in parenthesis, the maximum of the distribution**

| System | Potential(1) | Potential(2) | EXAFS K-Edge[2] | EXAFS L-Edge[2] | XANES[15] |
|---|---|---|---|---|---|
| $La^{3+}$ | 2.57 (2.52) | 2.50 (2.48) | 2.507 (2.484) | 2.486 (2.465) | 2.49 |
| $Gd^{3+}$ | 2.42 (2.41) | 2.38 (2.37) | 2.388 (2.381) | 2.388 (2.381) | 2.40 |
| $Lu^{3+}$ | 2.36 (2.34) | 2.33 (2.32) | 2.297 (2.287) | 2.288 (2.282) | 2.29 |

Concluding, we should remark that experiments report a decrease in Ln-O distances between $La^{3+}$ and $Gd^{3+}$ of about 0.1 Å and between $Gd^{3+}$ and $Lu^{3+}$ in the 0.05–0.07 Å range and the two potentials reproduce this quantity relatively well (with small deviations), providing about 0.1 Å in both cases. While both potentials provide that 8 DMSO are in the first coordination shell of $Lu^{3+}$ and $Gd^{3+}$, in the $La^{3+}$ case both potentials lead to a fractional coordination number arising from the coexistence of an 8-fold and a 9-fold geometry for the first solvation shell. Since the contradictory experimental evidence[2,30] accumulated so far is not sufficient to unambiguously determine a unique structure characterizing the first solvation shell we report in the following the geometrical features of both the possibilities.

## $La^{3+}$@DMSO solvation structure

As reported previously (see the coordination numbers plot in Figure 2), the two model potentials, (1) and (2), provide for $La^{3+}$ both CN=9 and CN=8 solvation structures. We now analyze in more details such simulations to characterize the two possible coordination structures. From the dynamical point of view we can see from the time dependent La-

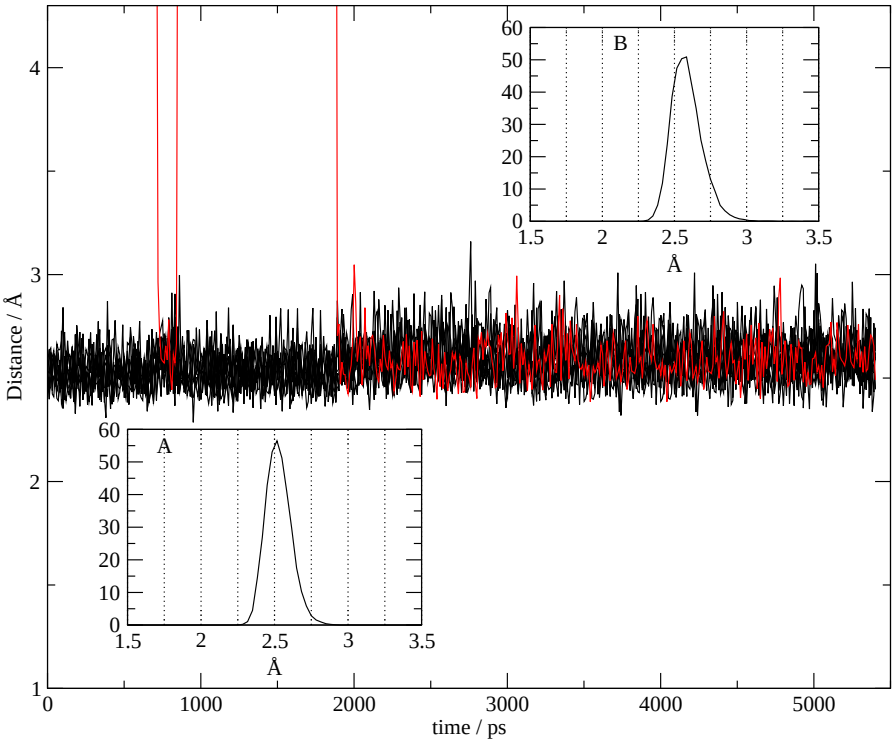


Figure 3: La-O distances as a function of simulation time in the $La^{3+}$-DMSO system

O distances reported in Figure 3 calculated with potential (1) that there is a dynamical exchange between the configuration with CN=8 and that with CN=9. In this figure, only the La-O distances smaller than 4 Å are reported. The first eight molecules are shown in black and the ninth molecule that moves from second to first shell is shown in red. The two insets show the RDFs calculated on two different portions of the dynamics: one (A) calculated on the portion going from 1 to 1500 ps (characterized by a shell of 8 molecules) and the second (B) calculated on the portion ranging from 2500 to 5000 ps. When the ninth molecule is part of the first coordination shell we can see that the distribution of La-O distances broadens and its barycenter shifts to larger distances from 2.53 Å to 2.59 Å.

In order to check the sensitivity of our calculations to the initial conditions, we have run two additional dynamics (of approximately 5 ns each) starting respectively from a configuration with 9 and 8 oxygen atoms in the first shell. In both cases we have obtained a dynamical behavior where the dominant structure turned out to be the configurations with 9 atoms in

the first shell and coordination numbers around 8.9. We conclude that the dynamics carried out using potential (1) tend to have a net preference for a 9-fold solvation shell of $La^{3+}$.

We show in Figure 4, in a similar fashion to what we did in Figure 3, for potential (1) the evolution of the coordination shell for potential (2). As we can see, even with a potential that has a smaller vdW radius for the central ion and that produces a radial distribution in very good agreement with experiments, we have a coexistence of 9 and 8-fold coordination motifs. In Figure 4 we see (in green and in red) molecules moving from the solvation shell to the bulk and from the bulk to the first coordination shell.

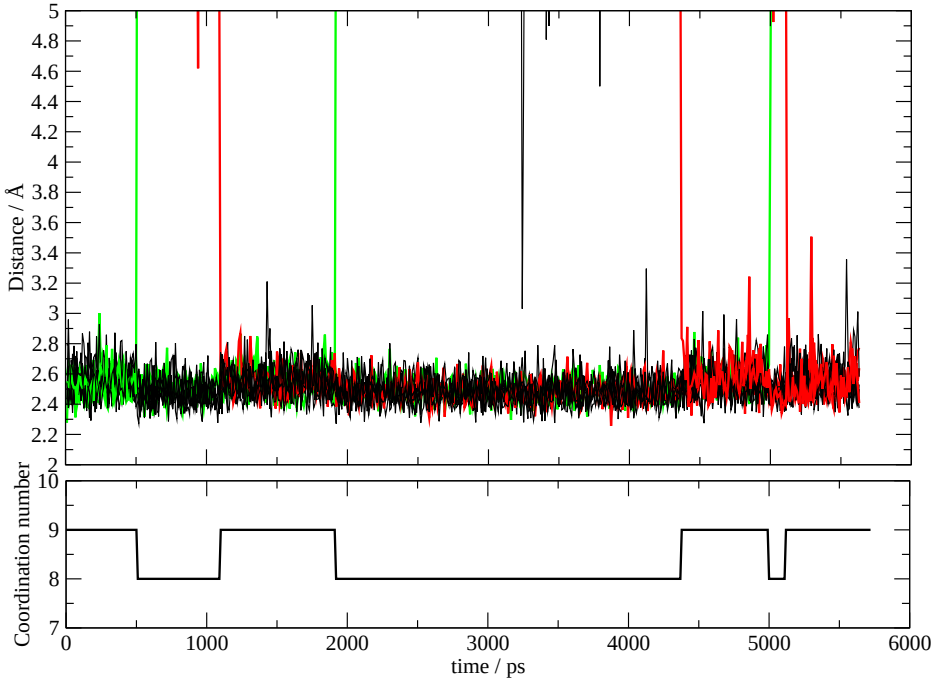


Figure 4: Upper panel: La-O distances as a function of simulation time in the $La^{3+}$-DMSO system. Lower panel: coordination number as a function of time. See main text for details.

We now describe the shapes and geometry of the two coordination models that we have found in our simulations. We shall use the data coming from potential (1), but those coming from potential (2) are quite similar in terms of geometric shape and we shall not present them for sake of brevity. It is well known that one of the most common shapes in complexes with 8 ligands is the square antiprism, in particular for lanthanoid(III) ions.[1,11,28,61] The question

whether or not the first shell maintains a regular shape when coordinating 8 molecules can be partially answered by examining the geometric distribution around the ionic center. This is done in Figure 5 where we show the O-O RDF (on the left), and the angular distribution function between two vectors pointing from the central $La^{3+}$ ion to two oxygen atoms (on the right). The data on the left is presented as an average over the entire trajectory of Figure 3 (black), an average over the trajectory portion where $La^{3+}$ is 8-fold coordinated (red) and finally and average over the part of trajectory where the ion is 9-fold coordinated (blue). Apart of the "intensity" of the first peak, the profiles of the RDFs are very similar thereby leading us to conclude that the distances between the oxygen atoms remain substantially the same during the dynamics regardless of the local structure of the first coordination shell. On the other hand the data reported in the right panel of Figure 5 show a much more interesting behavior. In the upper right panel we show (solid red line) the angular distribution of all the possible O-La-O angles in the first coordination shell as obtained on the portion of trajectory which sees 8 molecules in the first shell. We also report the same angular distribution in a model cluster that has a square antiprism shape (dashed red line). We can see that the main features of a square antiprism are present in the simulation although the conformation in the liquid seems to be less structured. In particular the distribution of the liquid phase shows two peaks around 70° and 140°. The former corresponds to the angles between adjacent oxygen atoms in one of the two squares or between atoms on two different squares but joined by an edge. The latter instead is the angle formed by atoms located on different squares, but not connected by an edge. Further inspection of Figure 5 shows that in the liquid we do not see the peak centered around 120° which corresponds to angles between atoms located on the same square ring but in opposite positions (i.e. those joined by a diagonal of the square). This effect is probably due to a sizable distortion of the antiprismatic structure during the dynamics. The situation is different for the CN=9 structure that is shown in terms of its angular distribution in the bottom-right panel of Figure 5. This CN=9 structure is that of a distorted square anti-prism with a cap corresponding to the additional oxygen atom. The

structure in the liquid matches almost perfectly that of the model system.

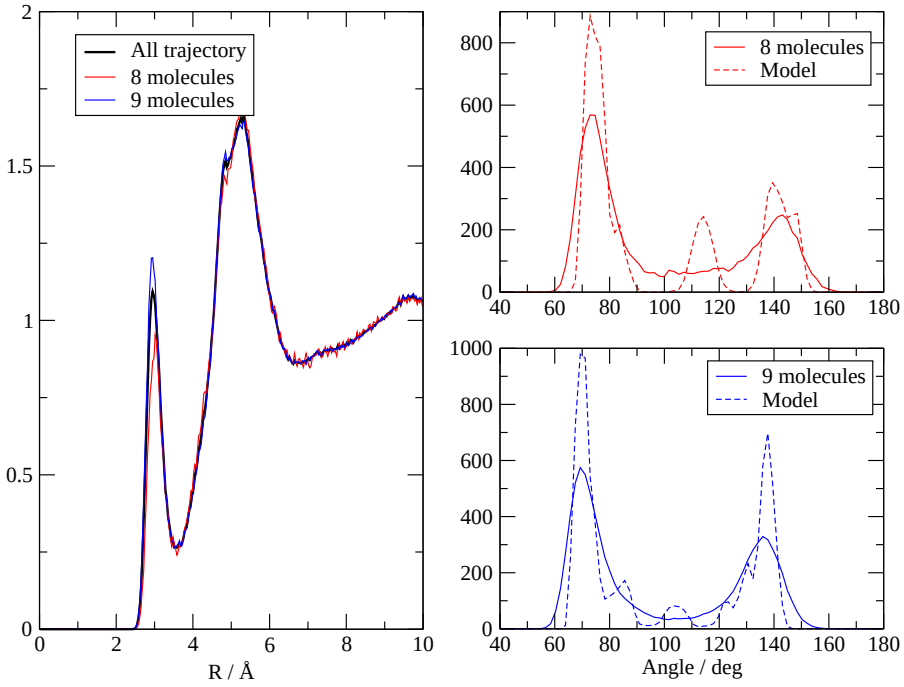


Figure 5: Left: O-O RDF on different portion of the trajectory. Right: O-La-O angular distributions on different portion of trajectory. See text for details.

In order to better elucidate the local geometry around the central ion we report in figure 6 the spatial distribution functions of the oxygen atoms of the first shell taken with respect to a three atom reference system that includes $La^{3+}$ and two of the surrounding oxygen atoms. The distribution functions have been evaluated on two trajectory portions of similar lengths where the system clearly shows a unique coordination number. More specifically the data collected for the coordination number equal to 8 refers to an average over the portion of the trajectory from 1 to 1500 ps (see Figure 3) and the data collected for the coordination number 9 stem from an average over the frames from 2500 to 5000 ps. In both cases the simulation time is enough to have equilibrated and converged structural results, such that the different time sampled for the two structures should not be relevant in providing spatial distribution function and other geometrical data (and 1.5 ns is the longest continuous portion with CN=8 we have in $La^{3+}$ trajectories). To allow for a simple comparison we also report

the model systems from which we have taken the angular distributions above. As we can see the structure with CN=8 is fairly regular in the dynamic simulation and clearly looks like the square antiprimastic structure of the model. On the other hand the structure with CN=9, albeit still very similar to the model, shows a certain degree of disorder due to increased motion of the oxygen atoms around their equilibrium positions. By comparing the structures obtained with MD and those arising from the models we conclude that the CN=9 geometry is a square antiprism with a ninth oxygen atom that forms a cap on one of the square faces.

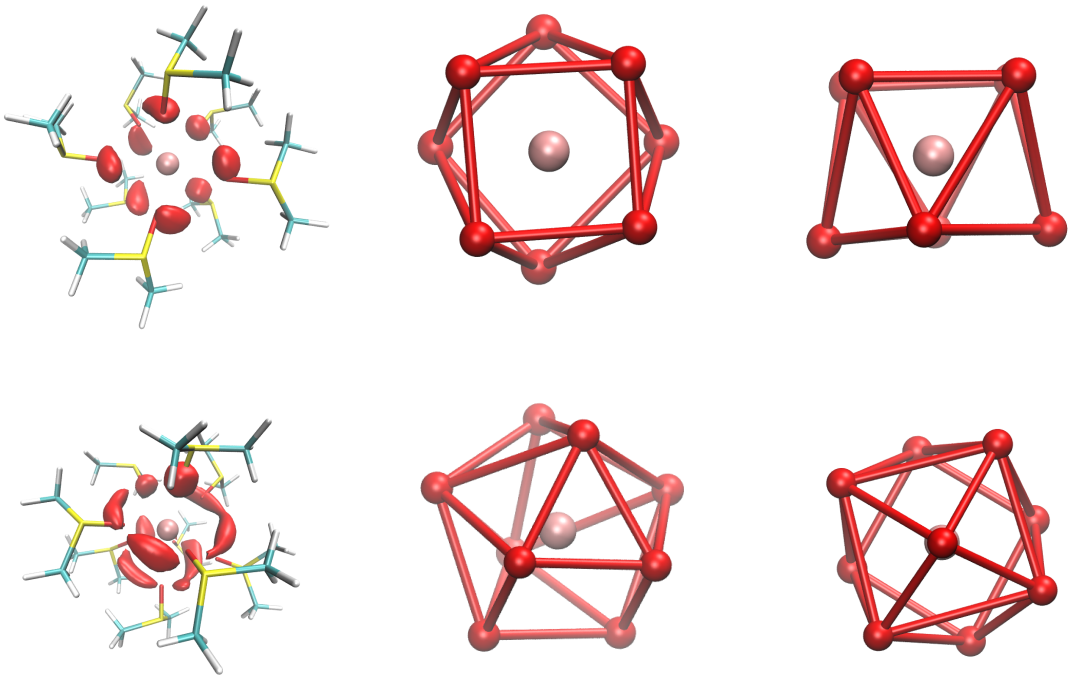

Figure 6: Left panels: spatial distribution functions around the central $La^{3+}$ ion from MD. Central and right panels: model geometrical systems from two different points of view.

## $La^{3+}$@DMSO energetic

Finally, to better understand the possible coexistence of the 8- and 9-fold solvation structure, we have performed energetic calculations, both in the gas and liquid phase, using the potential (2), which better agrees with experiments in terms of La-O distance. In terms of

total internal energy, an isolated cluster containing 9 molecules directly bound to the central ion is more stable than the cluster obtained by moving one of the nine molecules in second shell (a configuration that we shall call 8+1, see Figure 2 in the supporting informations). In particular the energy difference between the minima of the 9 and 8+1 structures as computed using potential (2) turns out to be -3.17 kcal/mol (thus in favor of the 9 structure). If we now let the $r^0$ potential parameter to vary continuously between 3.4 and 4 Å and we calculate the energy difference between the minima of the 9 and 8+1 structures versus $r^0$ we find that the $\Delta E$ becomes positive (thereby favoring the 8+1 structure) when $r^0$ is sufficiently small i.e. 3.7 Å, a value that falls near the $Gd^{3+}$ parameter set (see Table 1). The energy as a function of $r^0$ is reported in Figure 1 of the supporting informations. These findings qualitatively justify the coordination numbers and the shapes of the solvation shells of the elements that we have analyzed above.

The competition between the 8-fold and the 9-fold coordination motifs in solution needs the calculation of free energy in solution. We have employed umbrella sampling molecular dynamics using the La-O distance as reaction coordinate to estimate the difference between the two coordination geometries. In particular, starting from a 9-fold structure, we gradually removed one DMSO molecule by increasing the La-O distance up to the point of obtaining an 8-fold structure that is the equivalent of the 8+1 gas phase structure. The resulting PMF is shown in Figure 7 where we have chosen $r_0 = 2.55$ Å in Eq. 5. The final free energy difference turns out to be in favor of the 9-fold structure of about 1.5 kcal/mol. This value is less than half of the gas phase value. The qualitative picture emerging from energy calculation is that both structures are thermally accessible.

## $Lu^{3+}$@DMSO and $Gd^{3+}$@DMSO solvation structure

In the case of heavier lanthanoid(III) ions the CN=8 coordination motif is the only one observed. In addition, we did not record any exchange between the first solvation shell and the bulk during the 4 ns dynamics. We now analyze in details such structures to clearly

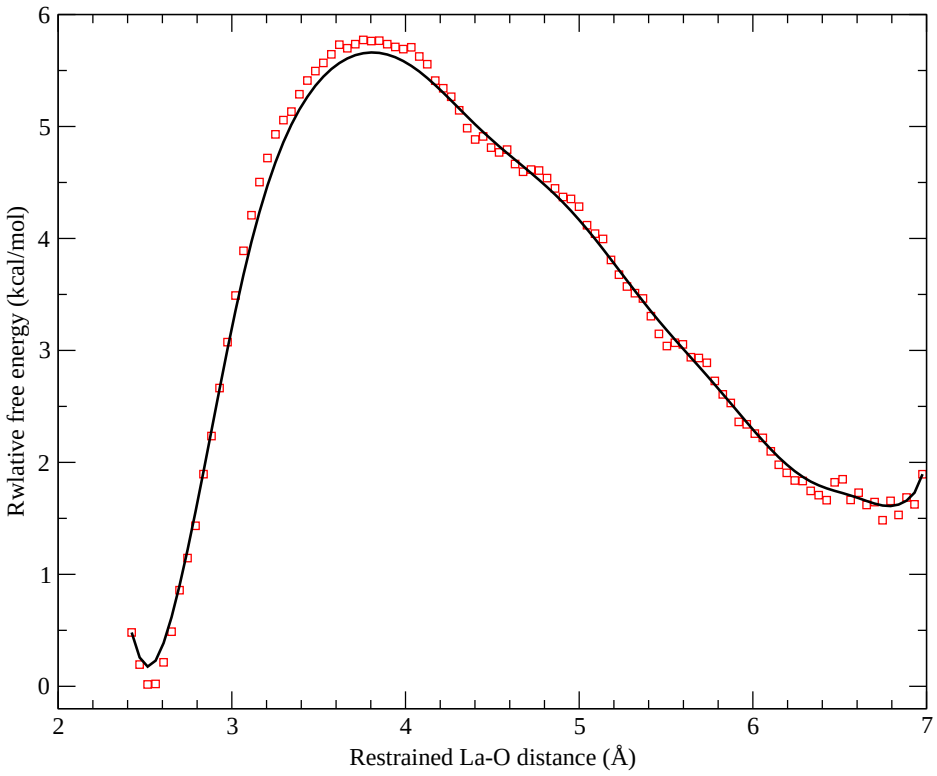


Figure 7: Free energy profile (PMF) for the extraction of one DMSO molecule from the $La^3$+@DMSO configuration with 9 molecules in the first shell. Raw data are shown as points and a smoothing interpolation is also shown as a guide for the eye.

define the arrangement of DMSO molecules around the central $Ln^{3+}$ ion. The radial and angular distributions for the O-O distance and O-Ln-O angles for both $Lu^{3+}$ and $Gd^{3+}$ ions are reported in Figure 8. In this figure we have collected only data coming from the oxygen atoms of the first shell without including those atoms which are farther than 3.5 Å from the ion. In a model cubic antiprism we have four sets of possible O-O distances that, in order of their lengths from the smallest to the largest, are: (i) those that connect atoms on two different square faces along an edge, (ii) those that connect two adjacent atoms along the side of the square faces, (iii) those that connect two opposite atoms across the square faces (along their diagonal) and (iv) those that connect atoms in two different square faces and non connected by and edge. We therefore expect to find 4 peaks in the (intra-shell) RDF of the oxygen atoms. In our simulation we find only two: the first peak (that is the more intense of the two) is actually made by the recurring distances that pertains to the (i) and (ii) groups above and the second peak is made by the recurrences of the (iv) group of distances. The group (iii) is missing. This is analogous to what we have noticed in the angular distribution functions reported above for $La^{3+}(DMSO)_8$ in Figure 5 where the angular peaks expected for the angles between oxygen atoms on two different squares but not connected by and edge was missing. Again, in the case of the other $Ln^{3+}$ ions we have a fairly regular square antiprism structure where however, internal motions distorts the two square faces thereby suppressing the occurrence of certain angular or distance recurrences between the oxygen atoms.

# Conclusions

We have studied how DMSO molecules are arranged around $Ln^{3+}$ ions by means of polarizable molecular dynamics simulations. To this end we have derived new vdW potential parameters for the Amoeba force field from quantum chemistry calculations on $La^{3+}$ and $Lu^{3+}$ clusters. Through an extrapolation procedure, taking advantage of the ionic radius

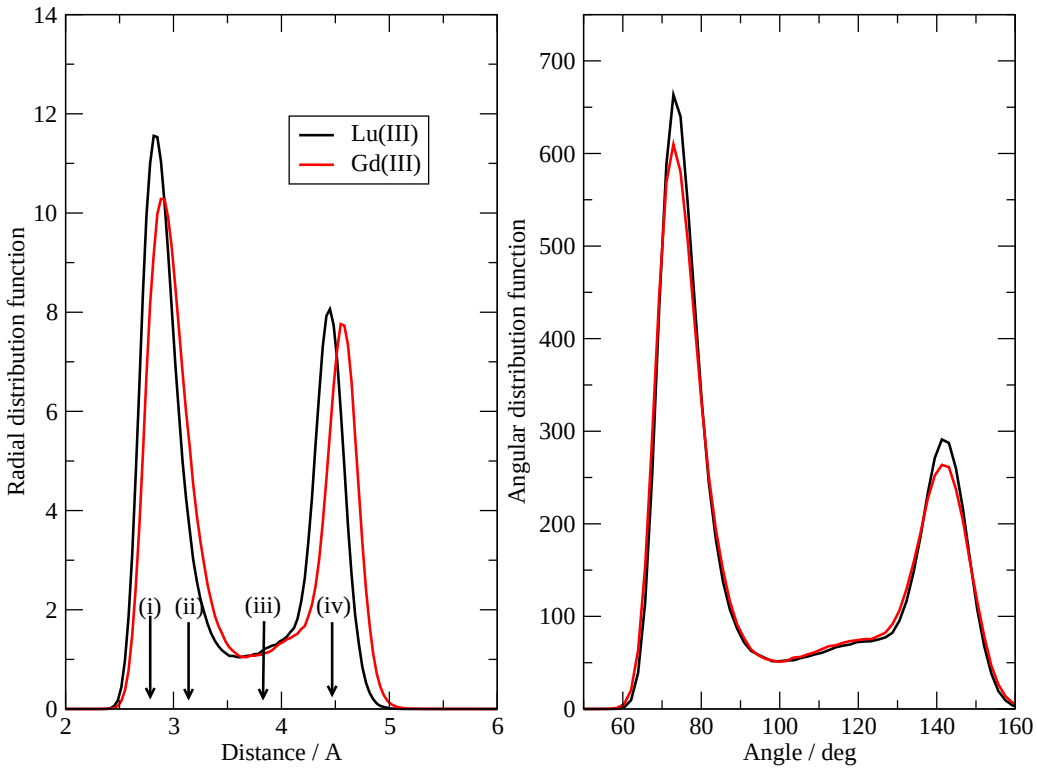


Figure 8: Left: O-O RDF for $Lu^{3+}$ and $Gd^{3+}$ in the first solvation shell. Right: O-La-O angular distributions. See text for details.

linear decrease across the series and similarly to what has been done for lanthanoids(III) in water,[14,21] it was possible to successfully determine the $Gd^{3+}$ force field parameters without additional quantum chemistry calculations. This *ab initio* based force field was able to correctly describe the distance decreasing across the series, although, in order to improve the ion-DMSO distance to match EXAFS and XANES data,[2,15,62] we had to slightly alter one of the potential parameter. For that, we had to pay the price of loosing accuracy with respect to cluster *ab initio* results.

Concerning the coordination number, in the case of heavy lanthanoids ($Gd^{3+}$ and $Lu^{3+}$) we obtain an 8-fold coordination, in agreement with EXAFS and XANES experiments.[2,15,62] In the case of $La^{3+}$, the situation seems to be less clear: both with the *ab initio* based and with the *rescaled* potential we obtain a mixed first shell configuration that includes a SAP 8-fold structure and a mono-capped SAP, 9-coordinated structure. Since the experimental determination of CN is not always very easy and free from uncertainty, the question weather a 8-fold or 9-fold structure is present when $La^{3+}$ is immersed in DMSO is still open. It is therefore likely that, similarly to what observed in $Ln^{3+}$ hydration,[63] there can be a dynamical coexistence of the two coordination schemes. Our free energy calculations also leave the possibility of a thermally induced oscillation open.

Finally, we have clearly determined that the 8-fold structures are thermally distorted square anti-prism structures, and the 9-fold structures are a square anti-prism to which a ninth molecule is added on one of the square faces. This picture is in agreement with the possible statistical coexistence of the two structures and with the difficulty of clearly determine the presence of such a ninth labile molecule in EXAFS and XANES experiments.

## Acknowledgement

Financial support of the Scientific Committee of the University of Rome through grant "Ricerca 2014" and of ANR 2010 JCJC 080701 ACLASOLV (Actinoids and Lanthanoids Solvation) are acknowledged. The support through grant "IscrB_METIL" of CINECA su-

percomputing centers and GENCI (grant x2015082484) are also acknowledged.

## Supporting Information Available

We supply a template of the parameter file to be used with the *tinker* package that contains the force field used in this work. The default units are kcal/mol and Å. This material is available free of charge via the Internet at `http://pubs.acs.org/`.

## References

(1) D'Angelo, P.; Spezia, R. Hydration of Lanthanoids(III) and Actinoids(III): An Experimental/Theoretical Saga. *Chem. Eur. J.* **2012**, *18*, 11162–11178.

(2) Persson, I.; Damian Risberg, E.; D'Angelo, P.; De Panfilis, S.; Sandström, M.; Abbasi, A. X-ray Absorption Fine Structure Spectroscopic Studies of Octakis(DMSO)lanthanoid(III) Complexes in Solution and in the Solid Iodides. *Inorg. Chem.* **2007**, *46*, 7742–7748.

(3) Binnemans, K. Lanthanides and Actinides in Ionic Liquids. *Chem. Rev.* **2007**, *107*, 2592–2614, PMID: 17518503.

(4) Ohtaki, H.; Radnai, T. Structure and Dynamics of Hydrated Ions. *Chem. Rev.* **1993**, *93*, 1157–1204.

(5) Helm, L.; Merbach, A. E. Inorganic and Bioinorganic Solvent Exchange Mechanisms. *Chem. Rev.* **2005**, *105*, 1923–1960.

(6) Habenschuss, A.; Spedding, F. H. The Coordination (Hydration) of Rare Earth Ions in Aqueous Chloride Solutions from X-ray Diffraction. I. $TbCl_3$, $DyCl_3$, $ErCl_3$, $TmCl_3$ and $LuCl_3$. *J. Chem. Phys.* **1979**, *70*, 2797–2806.

(7) Habenschuss, A.; Spedding, F. H. The Coordination (Hydration) of Rare Earth Ions in Aqueous Chloride Solutions from X-ray Diffraction. II. $LaCl_3$, $PrCl_3$, and $NdCl_3$. *J. Chem. Phys.* **1979**, *70*, 3758–3763.

(8) Cossy, C.; Helm, L.; Merbach, A. E. Oxygen-17 Nuclear Magnetic Resonance Kinetic Study of Water Exchange on the Lanthanide(III) Aqua Ions. *Inorg. Chem.* **1988**, *27*, 1973–1979.

(9) Cossy, C.; Helm, L.; Powell, D. H.; Merbach, A. E. A Change in Coordination Number from Nine to Eight Along the Lanthanide(III) Aqua Ion Series in Solution: a Neutron Diffraction Study. *New J. Chem.* **1995**, *19*, 27–35.

(10) Lundberg, D.; Persson, I.; Eriksson, L.; D'Angelo, P.; De Panfilis, S. Structural Study of the N,N′-Dimethylpropyleneurea Solvated Lanthanoid(III) Ions in Solution and Solid State with an Analysis of the Ionic Radii of Lanthanoid(III) Ions. *Inorg. Chem.* **2010**, *49*, 4420–4432.

(11) Abbasi, A.; Damian Risberg, E.; Eriksson, L.; Mink, J.; Persson, I.; Sandström, M.; Sidorov, Y. V.; Skripkin, M. Y.; Ullström, A.-S. Crystallographic and Vibrational Spectroscopic Studies of Octakis(DMSO)lanthanoid(III) Iodides. *Inorg. Chem.* **2007**, *46*, 7731–7741.

(12) D'Angelo, P.; Zitolo, A.; Migliorati, V.; Persson, I. Analysis of the Detailed Configuration of Hydrated Lanthanoid(III) Ions in Aqueous Solution and Crystalline Salts by Using K- and L-3-Edge XANES Spectroscopy. *Chem. Eur. J.* **2010**, *16*, 684–692.

(13) Persson, I.; D'Angelo, P.; De Panfilis, S.; Sandstrom, M.; Eriksson, L. Hydration of Lanthanoid(III) Ions in Aqueous Solution and Crystalline Hydrates Studied by EXAFS Spectroscopy and Crystallography: the Myth of the Gadolinium Break. *Chem. Eur. J.* **2008**, *14*, 3056–3066.

(14) D'Angelo, P.; Zitolo, A.; Migliorati, V.; Chillemi, G.; Duvail, M.; Vitorge, P.; Abadie, S.; Spezia, R. Revised Ionic Radii of Lanthanoid(III) Ions in Aqueous Solution. *Inorg. Chem.* **2011**, *50*, 4572–4579.

(15) D'Angelo, P.; Migliorati, V.; Spezia, R.; De Panfilis, S.; Persson, I.; Zitolo, A. K-edge XANES Investigation of Octakis(DMSO)lanthanoid(III) Complexes in DMSO Solution and Solid Iodides. *Phys. Chem. Chem. Phys.* **2013**, *15*, 8684–8691.

(16) Villa, A.; Hess, B.; Saint-Martin, H. Dynamics and Structure of Ln(III)-Aqua Ions: A Comparative Molecular Dynamics Study Using ab Initio Based Flexible and Polarizable Model Potentials. *J. Phys. Chem. B* **2009**, *113*, 7270–7281.

(17) Kowall, T.; Foglia, F.; Helm, L.; Merbach, A. E. Molecular Dynamics Simulations Study of Lanthanides Ions $Ln^{3+}$ in Aqueous Solutions. Analysisof the Structure of the First Hydration Shell and of the Origin of Symmetry Fluctuations. *J. Phys. Chem.* **1995**, *99*, 13078–13087.

(18) Kowall, T.; Foglia, F.; Helm, L.; Merbach, A. E. Molecular Dynamics Simulations Study of Lanthanides Ions $Ln^{3+}$ in Aqueous Solutions Including Water Polarization. Change in Coordination Number from 9 to 8 Along the Series. *J. Am. Chem. Soc.* **1995**, *117*, 3790–3799.

(19) Floris, F. M.; Tani, A. A Study of Aqueous Solutions of Lanthanide Ions by Molecular Dynamics Simulation with Ab Initio Effective Pair Potentials. *J. Chem. Phys.* **2001**, *115*, 4750–4765.

(20) Duvail, M.; Spezia, R.; Vitorge, P. A Dynamical Model to Explain Hydration Behaviour Trough Lanthanide Series. *ChemPhysChem.* **2008**, *9*, 693–696.

(21) Duvail, M.; Vitorge, P.; Spezia, R. Building a Polarizable Pair Interaction Potential for Lanthanoids(III) in Liquid Water : a Molecular Dynamics Study of Structure and Dynamics of the Whole Series. *J. Chem. Phys.* **2009**, *130*, 104501.

(22) Ciupka, J.; Cao-Dolg, X.; Wiebke, J.; Dolg, M. Computational Study of Lanthanide(III) Hydration. *Phys. Chem. Chem. Phys.* **2010**, *12*, 13215–13223.

(23) Clark, A. E. Density Functional and Basis Set Dependence of Hydrated Ln(III) Properties. *J. Chem. Theory Comput.* **2008**, *4*, 708–718.

(24) Di Bernardo, P.; Zanonato, P. L.; Melchior, A.; Portanova, R.; Tolazzi, M.; Choppin, G. R.; Wang, Z. Thermodynamic and Spectroscopic Studies of Lanthanides(III) Complexation with Polyamines in Dimethyl Sulfoxide. *Inorg. Chem.* **2008**, *47*, 1155–1164.

(25) Cassol, A.; Di Bernardo, P.; Portanova, R.; Tolazzi, M.; Tomat, G.; Zanonato, P. Thermodynamics of Lanthanide(III) Complexation with Ethylenediamine in Dimethyl Sulfoxide. *J. Chem. Soc. Dalton Trans.* **1992**, *3*, 469–473.

(26) Cassol, A.; Choppin, G. R.; Di Bernardo, P.; Portanova, R.; Tolazzi, M.; Tomat, G.; Zanonato, P. L. Thermodynamics of Lanthanide(III) Complex Formation with Nitrogen-Donor Ligands in Dimethyl Sulfoxide. *J. Chem. Soc., Dalton Trans.* **1993**, 1695–1698.

(27) Comuzzi, C.; Di Bernardo, P.; Portanova, R.; Tolazzi, M.; Zanonato, P. Thermodynamics of Lanthanide(III) Complexation with Ethylenediamine in Dimethyl Sulfoxide. *Polyhedron* **2002**, *21*, 1385–1391.

(28) Näslund, J.; Lindqvist-Reis, P.; Persson, I.; Sandström, M. Steric Effects Control the Structure of the Solvated Lanthanum(III) Ion in Aqueous, Dimethyl Sulfoxide, and N,N‘-Dimethylpropyleneurea Solution. An EXAFS and Large-Angle X-ray Scattering Study. *Inor. Chem.* **2000**, *39*, 4006–4011, PMID: 11198854.

(29) Buenzli, J.; Metabanzoulou, J.; Froidevauz, P.; Lin, L. FT-IR and Fluorometric Investigation of Rare Earth and Metal Ion Solvation. 9. Evidence for a Coordination

Number Change Along the Lanthanide Series: FT-IR Investigation of the Solvates [Ln(NO3)3(DMSO)n] in Anhydrous Acetonitrile. *Inorg. Chem.* **1990**, *29*, 3875–3881.

(30) Warminska, D.; Wawer, J. Apparent Molar Volumes and Compressibilities of Lanthanum, Gadolinium and Lutetium Trifluoromethanesulfonates in Dimethylsulfoxide. *J. Chem. Thermodynamics* **2012**, *55*, 79–84.

(31) Bodo, E.; Chiricotto, M.; Spezia, R. Structural, Energetic and Electronic Properties of La(III)-DMSO Clusters. *J. Phys. Chem. A* **2014**, *118*, 11602–11611.

(32) Dang, L. X.; Rice, J. E.; Caldwell, J.; Kollman, P. A. Ion Solvation in Polarizable Water: Molecular Dynamics Simulations. *J. Am. Chem. Soc.* **1991**, *113*, 2481–2486.

(33) Hünenberger, P.; Reif, M. *Single-Ion Solvation: Experimental and Theoretical Approaches to Elusive Thermodynamic Quantities*; RSC theoretical and computational chemistry series; Royal Society of Chemistry, 2011.

(34) D'Angelo, P.; Migliorati, V.; Mancini, G.; Chillemi, G. A Coupled Molecular Dynamics and XANES Data Analysis Investigation of Aqueous Cadmium(II). *J. Phys. Chem. A* **2008**, *112*, 11833–11841.

(35) Duvail, M.; Souaille, M.; Spezia, R.; Cartailler, T.; Vitorge, P. Pair Interaction Potentials With Explicit Polarization for Molecular Dynamics Simulations of $La^{3+}$ in Bulk Water. *J. Chem. Phys.* **2007**, *127*, 034503.

(36) Ponder, J. W.; Wu, C.; Ren, P.; Pande, V. S.; Chodera, J. D.; Schnieders, M. J.; Haque, I.; Mobley, D. L.; Lambrecht, D. S.; Di Stasio, R. A. et al. Current Status of the AMOEBA Polarizable Force Field. *J. Phys. Chem. B* **2010**, *114*, 2549–2564, PMID: 20136072.

(37) TINKER - Software Tools for Molecular Design. `dasher.wustl.edu/tinker/`.

(38) Clavaguera, C.; Calvo, F.; Dognon, J.-P. Theoretical Study of the Hydrated $Gd^{3+}$ ion: Structure, Dynamics, and Charge Transfer. *J. Chem. Phys.* **2006**, *124*, 074505.

(39) Clavaguera, C.; Sansot, E.; Calvo, F.; Dognon, J.-P. Gd(III) Polyaminocarboxylate Chelate: Realistic Many-Body Molecular Dynamics Simulations for Molecular Imaging Applications. *J. Phys. Chem. B* **2006**, *110*, 12848–12851.

(40) Piquemal, J.-P.; Perera, L.; Cisneros, G. A.; Ren, P.; Pedersen, L. G.; Darden, T. A. Towards Accurate Solvation Dynamics of Divalent Cations in Water Using the Polarizable Amoeba Force Field: from Energetics to Structure. *J. Chem. Phys.* **2006**, *125*, 054511.

(41) Zhang, J.; Yang, W.; Piquemal, J.-P.; Ren, P. Modeling Structural Coordination and Ligand Binding in Zinc Proteins with the AMOEBA Polarizable Potential. *J. Chem. Theo. Comput.* **2012**, *8*, 1314–1324.

(42) Ren, P. Y.; Ponder, J. W. Consistent Treatment of Inter- and Intramolecular Polarization in Molecular Mechanics Calculations. *J. Comput. Chem.* **2002**, *23*, 1497–1506.

(43) Ren, P. Y.; Wu, C. J.; Ponder, J. W. Polarizable Atomic Multipole-Based Molecular Mechanics for Organic Molecules. *J. Chem. Theory Comput.* **2011**, *7*, 3143–3161.

(44) Shi, Y.; Wu, C. J.; Ponder, J. W.; Ren, P. Y. Multipole Electrostatics in Hydration Free Energy Calculations. *J. Comput. Chem.* **2011**, *32*, 967–977.

(45) Jiao, D.; Golubkov, P. A.; Darden, T. A.; Ren, P. Y. Calculation of Protein–Ligand Binding Free Energy by Using a Polarizable Potential. *Proc. Natl. Acad. Sci. U. S. A.* **2008**, *105*, 6290–6295.

(46) Jiao, D.; Zhang, J. J.; Duke, R. E.; Li, G. H.; Schnieders, M. J.; Ren, P. Y. Trypsin Ligand Binding Free Energies from Explicit and Implicit Solvent Simulations with Polarizable Potential. *J. Comput. Chem.* **2009**, *30*, 1701–1711.

(47) Souaille, M.; Loirat, H.; Borgis, D.; Gaigeot, M.-P. MDVRY: A Polarizable Classical Molecular Dynamics Package for Biomolecules. *Comp. Phys. Comm.* **2009**, *180*, 276–301.

(48) Martelli, F.; Jeanvoine, Y.; Vercouter, T.; Beuchat, C.; Vuilleumier, R.; Spezia, R. Hydration Properties of Lanthanoid(III) Carbonates Complexes in Liquid Water by Polarizable Molecular Dynamics Simulations. *Phys. Chem. Chem. Phys.* **2014**, *16*, 3693–3705.

(49) Thole, B. T. Molecular Polarizabilities Calculated with a Modified Dipole Interaction. *Chem. Phys.* **1981**, *59*, 341–350.

(50) Roux, B. The Calculation of the Potential of Mean Force Using Computer Simulations. *Comp. Phys. Comm.* **1995**, *91*, 275–282.

(51) Grossfield, A. WHAM: The Weighted Histogram Analysis Method, Version 2.0.9. `http://membrane.urmc.rochester.edu/content/wham`.

(52) Caleman, C.; Hub, J. S.; van Maaren, P. J.; van der Spoelb, D. Atomistic Simulation of Ion Solvation in Water Explains Surface Preference of Halides. *Proc Natl Acad Sci* **2011**, *108*, 6838–6842.

(53) Neumann, R. M. Entropic Approach to Brownian Movement. *Am. J. Phys.* **1980**, *48*, 354–357.

(54) Vishnyakov, A.; Lyubartsev, A. P.; Laaksonen, A. Molecular Dynamics Simulations of Dimethyl Sulfoxide and Dimethyl Sulfoxide+Water Mixture. *J. Phys. Chem. A* **2001**, *105*, 1702–1710.

(55) Martelli, F.; Vuilleumier, R.; Simonin, J.-P.; Spezia, R. Varying the Charge of Small Cations in Liquid Water : Structural, Transport and Thermodynamical Properties. *J. Chem. Phys.* **2012**, *137*, 164501.

(56) Martelli, F.; Abadie, S.; Simonin, J.-P.; Vuilleumier, R.; Spezia, R. Lanthanoids(III) and Actinoids(III) in Water: Diffusion Coefficients and Hydration Enthalpies from Polarizable Molecular Dynamics Simulations. *Pure Apple. Chem.* **2013**, *85*, 237–246.

(57) Clavaguéra, C.; Dognon, J. Accurate Static Electric Dipole Polarizability Calculations of +3 Charged Lanthanide Ions. *Chem. Phys.* **2005**, *311*, 169 – 176, Relativistic Effects in Heavy-Element Chemistry and Physics. In Memoriam Bernd A. Hess (1954–2004).

(58) Jorgensen, W. L.; Maxwell, D. S.; Tirado-Rives, J. Development and Testing of the OPLS All-Atom Force Field on Conformational Energetics and Properties of Organic Liquids. *J. Am. Chem. Soc.* **1996**, *117*, 11225–11236.

(59) Cao, X.; Dolg, M. Pseudopotential Study of Lanthanum and Lutetium dimers. *Theor. Chem. Acc.* **2002**, *108*, 143–149.

(60) Shannon, R. D. Revised Effective Ionic Radii and Systematic Studies of Interatomic Distances in Halides and Chaleogenides. *Acta Crist. A* **1976**, *32*, 751–767.

(61) Burdett, J. K.; Hoffmann, R.; Fay, R. C. Eight-coordination. *Inorg. Chem.* **1978**, *17*, 2553–2568.

(62) Näslund, J.; Lindqvist-Reis, P.; Persson, I.; Sandström, M. Steric Effects Control the Structure of the Solvated Lanthanum(III) Ion in Aqueous, Dimethyl Sulfoxide, and *N,N'*-Dimethylpropyleneurea Solution. An EXAFS and Large-Angle X-ray Scattering Study. *Inorg. Chem.* **2000**, *39*, 4006–4011.

(63) Spezia, R.; Duvail, M.; Vitorge, P.; D'Angelo, P. Molecular Dynamics to Rationalize EXAFS Experiments: a Dynamical Model Explaining Hydration Behaviour Across the Lanthanoid(III) Series. *J. Phys.: Conf. Ser.* **2009**, *190*, 012056.

# Graphical TOC Entry

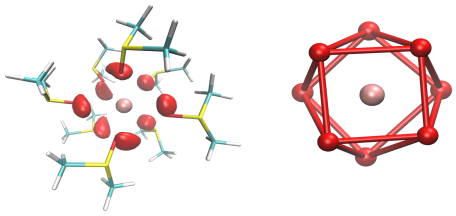

First shell of solvation of $Ln^{3+}$ ion immersed in DMSO as predicted by our models (left) and model structure (right).